

Vanda Grubišić\* and Ming Xiao  
Desert Research Institute, Reno, NV

## 1. INTRODUCTION

Very little is known climatologically about the frequency, temporal distribution, origin and strength of westerly wind events in the lee of the Sierra Nevada. Some of these events are associated with mountain wave activity generated by the Sierra Nevada that can lead to various degree of penetration of westerly momentum to the ground on the lee side (Cairns and Corey 2003; Grubišić and Billings 2006a). The local wind known as Washoe Zephyr (Twain 1871; Siscoe 1974), which tends to occur in the afternoon hours in summer, is thought to represent another type of the Sierra Nevada westerly wind event (Kingsmill 2000; Clements and Zhong 2005).

In this paper we present preliminary results of the climatology of westerly wind events in Owens Valley to the lee of the southern Sierra Nevada. This climatology is constructed using data from the mesonet of sixteen automatic weather stations in Owens Valley that was installed by DRI for the Sierra Rotors Project in 2004, and which has been in continuous operation since that time. The focus of this study is on the westerly wind events associated with the Sierra Nevada mountain lee waves for which a satellite-based climatology has been recently compiled (Grubišić and Billings 2006b).

## 2. INSTRUMENTATION and DATA

The SRP was the first, exploratory phase of a large coordinated effort to study atmospheric rotors, the second phase of which is the recently completed Terrain-induced Rotor Experiment (Grubišić et al. 2004; Grubišić and Doyle 2006). The goals of SRP have been, in part, to obtain climatological data on the locations and frequency of occurrence of rotors in Owens Valley to aide in the design of T-REX. Owens Valley is a narrow valley in eastern California, approximately north-south oriented and bounded by the highest portion of the Sierra Nevada (High Sierra) to the west and by the White-Inyo Range to the east. The DRI long-term network of 16 automatic weather stations (AWS) with telemetry located south of Independence in the central portion of Owens Valley was part of the core instrumentation deployed in SRP (Fig. 1). This network, which was also an integral part of the T-REX ground-based instrumentation suite, has been providing data in near real-time since the end of February 2004.

The 16 AWS of the DRI network are arranged in three approximately parallel rows. The average separation be-

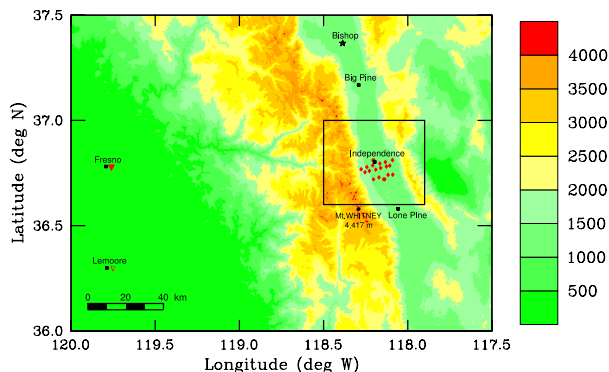


FIG. 1: The SRP field area with deployed major instrumentation marked with red symbols: i) DRI network (solid diamonds), ii) NCAR Integrated Sounding Systems (ISS) (solid circles), and iii) two atmospheric sounding systems: NCAR MGAUS (open down-pointing triangle), and a radiosonde unit at the Naval Air Station (NAS) Lemoore (filled down-pointing triangle). The box encloses the area shown in Fig. 2.

tween individual stations along these three lines is approximately 3 km (Fig. 2). Each station consists of a standard 30 ft (10 m) meteorological tower, and sensors for wind, temperature, relative humidity, and pressure. The stations' sensors are sampled every 3 seconds, and the data is temporally averaged over 30-second non-overlapping intervals. The temporally-averaged data is saved on the stations' data loggers before being sent via radio communication to the base station in Independence. From there, the data transfer to the central repository at DRI is carried over Internet, allowing near real-time online access to the graphically-displayed data (<http://www.wrcc.dri.edu/trex/>).

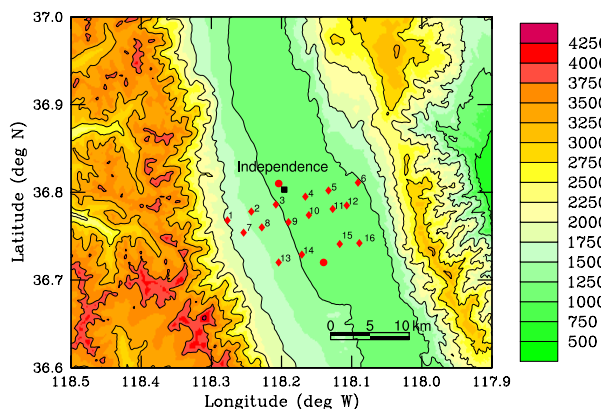


FIG. 2: DRI AWS ground network layout. Terrain height is shown in color.

\*Corresponding author's address: Dr. Vanda Grubišić, Desert Research Institute, Division of Atmospheric Sciences, 2215 Raggio Pkwy, Reno, NV 89512-1095; e-mail: Vanda.Grubic@dri.edu

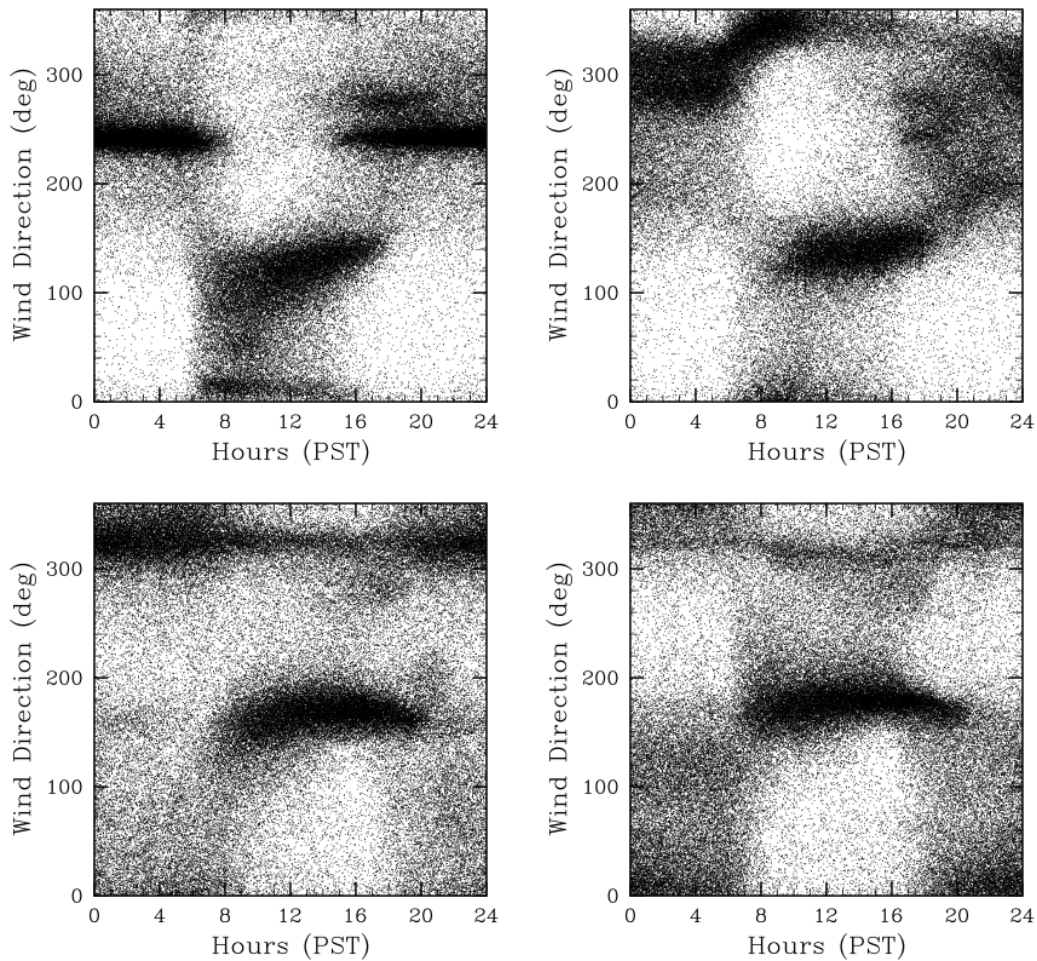


FIG. 3: Scatter diagrams of wind direction at wind speed  $> 1 \text{ m s}^{-1}$  as a function of time during the day. The data shown is from 10-min averages for period March 1, 2004 to May 31, 2006. Station 1 (top left), Station 9 (top right), Station 12 (bottom left), and Station 6 (bottom right).

### 3. FLOW REGIMES

#### 3.1 Diurnal Circulation Patterns

Diurnal thermally-forced circulation patterns at the DRI network stations are to a large degree determined by the valley geometry. The valley itself is about 150 km long and 15–30 km wide and oriented approximately north to south (mean valley axis orientation of 6 degrees W of N). In the cross-valley direction, the valley can be characterized with a wide U-shaped profile. The bottom of the valley ( $\sim 15 \text{ km}$  wide) consists of a flat, central part, and a gentle alluvial slope ( $< 5\%$ ) at the western end. The eastern Sierra and the western Inyo slopes (both close to 30%) raise steeply above the alluvial slope at the western end and almost directly from the flat bottom at the eastern end of the valley. The ridge-to-ridge width of the valley is nearly double its width at the bottom. Heterogeneity of the terrain in the along-valley direction is small across the network, but is more pronounced within distances of less than 5 km to the north and 10 km to the south of the network location. Within such a valley one expects two primary thermally-driven circulation patterns: 1) up- and

down-slope flow, and 2) up- and down-valley flow (Whiteman 1990).

Pattern 1 (up-slope flow during the day and down-slope at night) is primarily in evidence at five (5) stations of the network that lie on the alluvial slope (Group 1: stations 1, 2, 7, 8, and 13). An example of this pattern is shown in Fig. 3(top left) for Station 1 showing an unidirectional SW winds at night ( $\sim 240^\circ$ ), and a gradually turning up-slope SE flow during the day ( $\sim 100^\circ\text{--}140^\circ$ ). Pattern 2 (up-valley during the day and down-valley during the night) is most clearly in evidence at five (5) stations located in the central flats of the valley (Group 2: stations 5, 11, 12, 15, and 16; Fig. 3(bottom left)) showing the predominance of S-SE winds ( $\sim 160\text{--}180^\circ$ ) during the day, and N-NW winds ( $\sim 320^\circ\text{--}340^\circ$ ) at night. Two additional separate clusters of data points are also visible in these two panels: i) daytime N (Fig. 3(top left)) or NW winds (Fig. 3(bottom left)), and ii) late afternoon westerly winds (both). A transitional, hybrid pattern between Pattern 1 and Pattern 2 characterize stations on the border between the central flats and the alluvial slope (Group 3: stations 3, 4, 9, 10 and 14; Fig. 3(top right)). While to a certain degree the di-

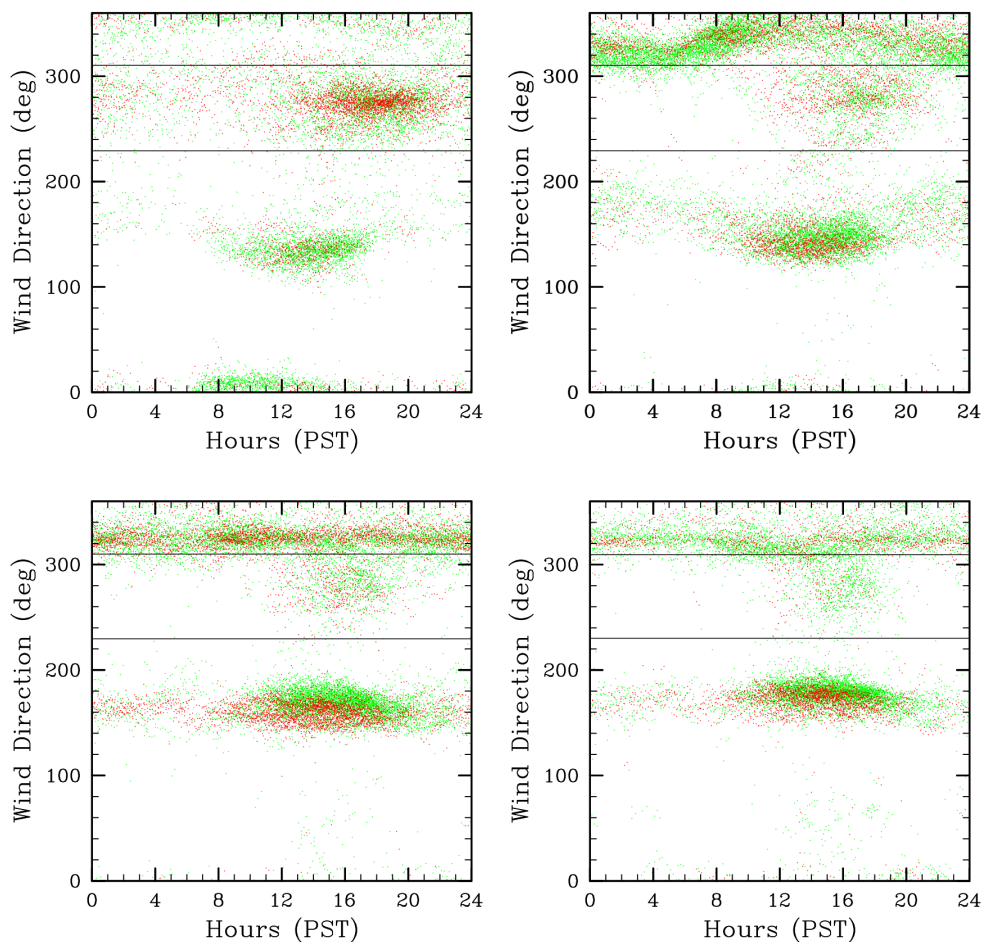


FIG. 4: Scatter diagram of wind direction for wind speed  $\in (7, 10] \text{ m s}^{-1}$  (green) and wind speed  $> 10 \text{ m s}^{-1}$  (red) as a function of time during the day. The data shown is 10-min average data for period March 1, 2004 to May 31, 2006. Station 1 (top left), Station 9 (top right), Station 12 (bottom left), and Station 6 (bottom right). Black horizontal lines mark the pair of wind directions  $270^\circ \pm 40^\circ$ .

urnal circulation pattern at Station 6, at the lower western Inyo slopes resembles that of Group 2, the predominance of N winds and a significantly higher scatter of nighttime wind directions (due to lower wind speeds) at this site has prompted us to place it in a separate group (Fig. 3(bottom right)).

The average strength of thermal circulation in the valley depends on the station location and the branch of the thermally-driven flow (daytime vs. nighttime). For example, the average speed of the nighttime downslope flow at stations in Group 1 (Pattern 1) is about  $4 \text{ m s}^{-1}$ , except for station 7 where it is slightly below  $3 \text{ m s}^{-1}$ , reflecting some micro characteristic of that location. The stations in Group 3 show similar wind speed characteristics to those in Group 1. For stations in Group 2 (Pattern 2), the difference in the strength of daytime and nighttime flows is more pronounced, with weaker nighttime (down-valley flows;  $\sim 3 \text{ m s}^{-1}$ ) and stronger daytime flows. In Fig. 4 we illustrate some of this variation with the scatter diagrams for wind direction for wind speed  $\in (7, 10] \text{ m s}^{-1}$  (green) and wind speed  $> 10 \text{ m s}^{-1}$  (red) at the same four stations shown in Fig. 3. The vigorous (in excess of  $10 \text{ m s}^{-1}$ ) up- and, in particular, down-valley flows at Group 2

and Group 3 stations, which can occur at any time of the day, are most likely evidence of flow channeling under a variety of synoptic conditions (Whiteman 1990). In addition to the above described features, a distinct cluster of westerly winds in the late afternoon hours is clearly visible at all station plots in Fig. 4. In the next section, we examine these westerly winds in more detail.

### 3.2 Westerly Wind Events

From the preceding analysis it is clear that westerly wind events represent a distinct class of wind events at all stations of the network. Our basic definition of a westerly wind event is that of  $WD \in [270^\circ \pm 40^\circ]$  and  $WS > 7 \text{ m s}^{-1}$  simultaneously occurring at stations 1 and 2 of the network. The distribution of these events throughout the day and through the year (Fig. 5(top left)) shows that they can occur at any time of the year but most frequently in the period from March through September. In cold winter months (Dec, Jan, Feb), the frequency of these events is significantly lower than at other times of the year. The westerly wind events during summer months (Jun, Jul, Aug) occur exclusively in the afternoon hours; those in other months can also extend late into the evening and

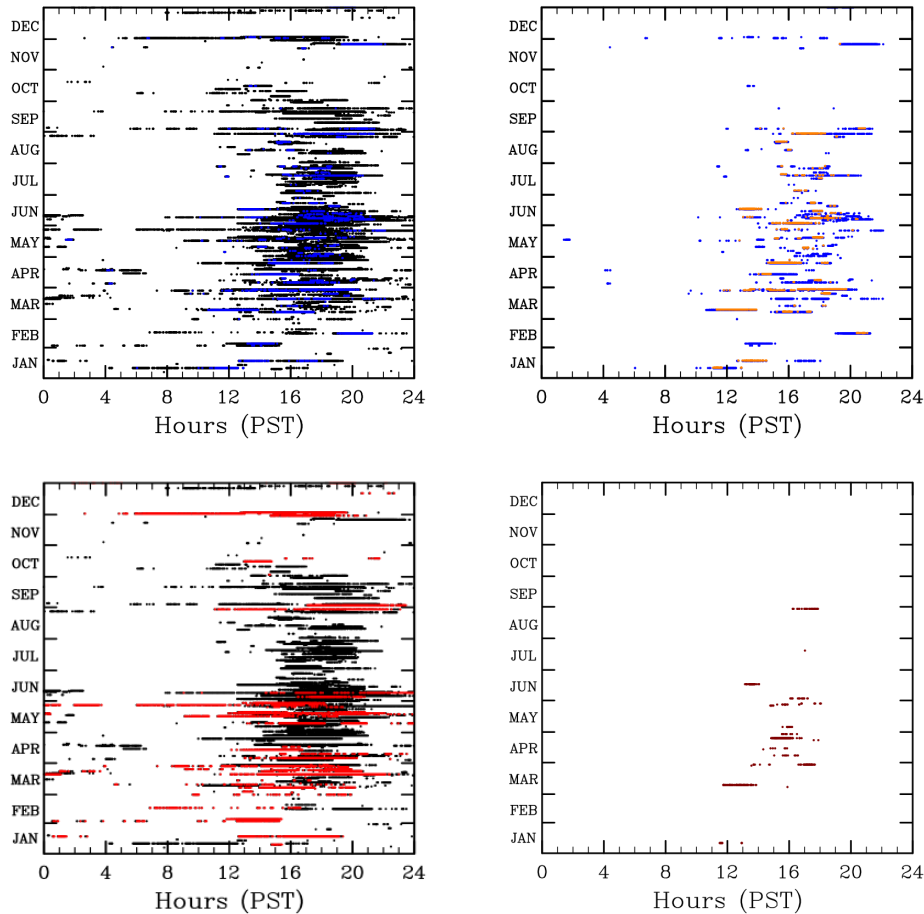


FIG. 5: Westerly wind events as a function of time during the day and time of the year (for the definition of westerly wind events see text). These diagrams were constructed using the 30-sec data from the period June 1, 2004 to May 31, 2006. Top left: Events recorded simultaneously at stations 1 and 2 (black) and at Group 1 stations (blue). Top right: Events at Group 1 stations (blue) and at Group 1 and Group 3 stations (orange). Bottom right: Events recorded simultaneously at all stations of the network. The data in this panel only is provided for the period March 1, 2004 to May 31, 2006 to include both the SRP and the T-REX field campaigns. Bottom left: Westerly wind events at stations 1 and 2 (black) and events for which the ridge-normal component of wind at 700 hPa was  $> 10 \text{ m s}^{-1}$  (red).

throughout the night.

As stations 1 and 2 are often reached by a gap jet originating in Kearsarge Pass (Grubišić and Billings 2006a) further constraining our definition of the westerly wind event to include all stations in Group 1 significantly reduces the number of events without significantly altering their distribution (blue dots in Fig. 5). By successively adding further constraints of the same wind conditions<sup>1</sup> occurring simultaneously at all stations in Group 1 and Group 3 (orange dots), and in Groups 1, 2, and 3 (not shown), we can see that only a small fraction of these events extend beyond the center of the valley. The bottom right panel of Fig. 5 shows events in which the westerly wind over  $7 \text{ m s}^{-1}$  was recorded simultaneously at all stations of the network in the period of March 1, 2004 to May 31, 2006, which includes both the SRP and the T-REX field campaigns in March and April 2004 and 2006,

<sup>1</sup>For all stations in Group 2 and a subset of stations in Group 3 the upper limit of the defining westerly wind direction interval was lowered to  $300^\circ$  to exclude flow channeling events.

respectively. Two SRP IOPs (IOP 12 on April 14, 2004, and IOP 16 on April 28, 2004), one non-IOP SRP period (on April 7, 2004), and one T-REX IOP (IOP 3 on Mar 9, 2006) are represented in this group. Clearly, the most intense westerly wind events occur in months with the highest frequency of mountain wave events (Grubišić and Billings 2006b).

To provide further quantitative evidence for this argument, for all westerly wind events that occurred simultaneously at stations 1 and 2 in the examined two-year period (black dots in Fig. 5(top left)) we have computed the component of the wind at 700 hPa normal to the Sierra ridge from the 00 UTC Oakland, CA upper-level soundings. While Oakland, CA is further north from our study area, this site has a more complete data record than the closer Vandenberg, CA upper-air sounding location. During summer months the ridge-normal component of the wind is low, well below the  $7.5\text{--}10 \text{ m s}^{-1}$  threshold that was used operationally during the T-REX campaign to identify time periods favorable for wave activity. On

the other hand, a number of events in the months from September through May, satisfy this condition. The scatter diagram for those westerly wind events at stations 1 and 2 for which the ridge-top winds in Oakland sounding are in excess of  $10 \text{ m s}^{-1}$  are shown in Fig. 5(bottom left).

#### 4. DISCUSSION and FUTURE WORK

Based on the analysis of slightly over two years of wind data from the DRI network in Owens Valley, CA, we have shown that westerly wind events represent a distinct class of events for all 16 stations of the network. These wind events occur throughout the year, most frequently in the period from March through September, predominantly in the afternoon hours. The frequency of the westerly wind events is significantly higher at stations that lie at the western end of Owens Valley at the foot of the eastern Sierra slopes, and in particular those along the valley exit of Kearsarge Pass (stations 1 and 2).

In summer months, the westerly wind events are limited to afternoon hours. The ridge-normal component of 700 hPa wind during these events is low, well below the empirically determined threshold required for mountain wave generation by the Sierra Nevada ( $7.5\text{--}10 \text{ m s}^{-1}$ ). Thus, the summertime lee side westerly events, some of which are quite vigorous and extend all the way to the eastern side of Owens Valley, are most likely the Washoe Zephyr events, which are believed to be driven by the regional pressure gradient that develops in summer between a thermal low over the Great Basin, and a high pressure area over the coastal California (Kingsmill 2000).

The number of lee side westerly wind events for which the ridge top wind is in excess of  $10 \text{ m s}^{-1}$  is significant in months from September through May, in particular from March through May, the months with the highest frequency of mountain wave events as evidenced in visible satellite imagery (Grubišić and Billings 2006b). While strong lee-side westerlies due to wave activity also tend to occur in the afternoon hours (Grubišić and Billings 2006a), our analysis shows they can appear earlier in the course of the day and extend well into the night.

The predominant occurrence of strong westerly wind events in Owens Valley in the lee of the Sierra Nevada in the afternoon hours from March through September points to the thermal forcing as a common forcing mechanism in both the Washoe Zephyr, where it is likely the primary mechanism, and strong mountain wave events in the lee of the Sierra Nevada, where it works in conjunction with the dynamical forcing (Kuettner 1959). The role of thermal forcing will be further investigated in our future analyses of T-REX wave and rotor events.

*Acknowledgments.* DRI mesonet network was installed and is maintained in collaboration with the DRI's Western Regional Climate Center (WRCC). We thank all those involved in the Sierra Rotors and the T-REX campaigns for their individual contributions. The Sierra Rotors and T-REX were funded by the National Science Foundation (NSF). This work was supported in part by NSF, Division of Atmospheric Sciences, Grants ATM-0242886 and ATM-0524891 to DRI.

#### 5. REFERENCES

- Cairns, M. M., and J. Corey, 2003: Mesoscale model simulations of high-wind events in the complex terrain of western Nevada. *Wea. Forecast*, **18**, 249–263.
- Clements, C., and S. Zhong, 2005: Daytime down-canyon flows in the eastern Sierra Nevada, California. *Proceedings. ICAM/MAP 2005*, Zadar, Croatia, <http://www.map.meteoswiss.ch/map-doc/icam2005/pdf/session-01/S1-04.pdf>
- Grubišić, V., J. D. Doyle, J. Kuettner, G. S. Poulos, and C. D. Whiteman, 2004: Terrain-induced Rotor Experiment. Scientific Overview Document and Experiment Design. 72 pp. Available at <http://www.atd.ucar.edu/projects/trex/documents>.
- Grubišić, V., and B. J. Billings, 2006a: Sierra Rotors: A comparative study of three mountain wave and rotor events. *Online Proceedings. 12<sup>th</sup> Conference on Mountain Meteorology*. Amer. Meteor. Soc. Paper **P2.4**
- Grubišić, V., and B. J. Billings, 2006b: Climatology of the Sierra Nevada mountain wave events. *Mon. Wea. Rev.*, Submitted.
- Grubišić, V., and J. D. Doyle, 2006: Terrain-induced Rotor Experiment (Invited). *Online Proceedings. 12<sup>th</sup> Conference on Mountain Meteorology*. Amer. Meteor. Soc. Paper **9.1**
- Kingsmill, D., 2000: Diurnally driven summertime winds in the lee of the Sierra: The Washoe Zephyr. *Preprints. Ninth Conference on Mountain Meteorology, Aspen, CO*. Amer. Meteor. Soc.
- Kuettner, J., 1959: The rotor flow in the lee of mountains. Geophysics Research Directorate (GRD) Research Notes 6, AFCRC-TN-58-626, Air Force Cambridge Research Center, USA, 20 pp.
- Siscoe, G. L., 1974: Mark Twain on weather. *Bull. Amer. Meteor. Soc.*, **55**, 4–8.
- Twain, M., 1871: *Roughing It*. New York: Harper and Brothers. 330 pp.
- Whiteman, C. D., 1990: Observations of thermally developed wind systems in mountainous terrain. Chapter 2 in *Atmospheric Processes Over Complex Terrain*, (W. Blumen, Ed.), *Meteorological Monographs*, **23**, no. 45., Amer. Meteor. Soc., Boston, Massachusetts, 5–42.